Monthly Notices of the ROYAL ASTRONOMICAL SOCIETY

Mon. Not. R. Astron. Soc. **410,** 1577–1582 (2011) doi:10.1111/j.1365-2966.2010.17539.x

Gamma-rays from molecular clouds illuminated by cosmic rays escaping from interacting supernova remnants

Yutaka Ohira,[1★] Kohta Murase[2,3] and Ryo Yamazaki[4]

[1]*Theory Centre, Institute of Particle and Nuclear Studies, KEK, 1-1 Oho, Tsukuba 305-0801, Japan*
[2]*Department of Physics, Tokyo Institute of Technology, 2-12-1, Ookayama, Meguro-ku, Tokyo 152-8550, Japan*
[3]*Center for Cosmology and AstroParticle Physics, 191, West Woodruff Avenue, Columbus, Ohio 43210, USA*
[4]*Department of Physics and Mathematics, Aoyama Gakuin University, 5-10-1 Fuchinobe, Sagamihara 252-5258, Japan*

Accepted 2010 August 15. Received 2010 August 15; in original form 2010 July 30

ABSTRACT

Recently, the gamma-ray telescopes *AGILE* and *Fermi* observed several middle-aged supernova remnants (SNRs) interacting with molecular clouds. It is likely that their gamma-rays arise from the decay of neutral pions produced by the inelastic collision between cosmic rays (CRs) and nucleons, which suggests that SNRs make the bulk of Galactic CRs. In this paper, we provide the analytical solution of the distribution of CRs that have escaped from a finite-size region, which naturally explains observed broken power-law spectra of the middle-aged SNRs. In addition, the typical value of the break energy of the gamma-ray spectrum, 1–10 GeV, is naturally explained from the fact that the stellar wind dynamics shows a separation between the molecular clouds and the explosion centre of about 10 pc. We find that the runaway-CR spectrum of the four middle-aged SNRs (W51C, W28, W44 and IC 443) interacting with molecular clouds could be the same, even though it leads to different gamma-ray spectra. This result is consistent with that of recent studies of Galactic CR propagation, and supports that SNRs are indeed the sources of Galactic CRs.

Key words: cosmic rays – ISM: individual objects: W51C – ISM: individual objects: W28 – ISM: individual objects: W44 – ISM: individual objects: IC 443 – ISM: supernova remnants.

1 INTRODUCTION

Supernova remnants (SNRs) are thought to be the origin of Galactic cosmic rays (CRs). The most popular acceleration mechanism at SNRs is diffusive shock acceleration (DSA; Axford, Leer & Skadron 1977; Krymsky 1977; Bell 1978; Blandford & Ostriker 1978). To make Galactic CRs, a few tens of per cent of the explosion energy of a supernova is converted to CR energy (Baade & Zwicky 1934). Recent gamma-ray telescopes, such as *Fermi* and *AGILE*, suggest that middle-aged SNRs interacting with molecular clouds likely emit hadronic gamma-rays, which arise from the decay of π^0 produced in inelastic collisions of the accelerated protons with molecular clouds (Abdo et al. 2009b, 2010a,b,c; Giuliani et al. 2010; Tavani et al. 2010). This fact supports that the SNRs make the bulk of Galactic CRs. *Fermi* observations revealed that the gamma-ray spectra of middle-aged SNRs have a broken power-law form, that the break photon energies are typically ∼1–10 GeV, and that the spectral indices above the break energy are different from each other.

Several theoretical interpretations of the gamma-ray observations of middle-aged SNRs have been proposed. Aharonian & Atoyan (1996) and Gabici, Aharonian & Casanova (2009) have investigated the gamma-ray spectrum from molecular clouds illuminated by CRs that have escaped from a nearby SNR. They showed that the spectrum is steeper than predicted by DSA at the shock because of the energy-dependent diffusion. In addition, Aharonian & Atoyan (1996) showed that the spectrum has a broken power-law form due to the finite size of the emission region. On the other hand, Malkov, Diamond & Sagdeev (2010) recently proposed a possible explanation. They claimed that in the partially ionized medium, CRs accelerated at the shock have a broken power-law spectrum – above the break energy, the damping of waves that resonantly scatter the CRs is significant, making a steeper spectrum than below the break energy.

In this paper, we propose another explanation for the observed middle-aged SNRs interacting with molecular clouds, by reinvestigating the distribution of CRs that have escaped from an SNR. So far, the point-source approximation has been widely adopted. However, for SNRs interacting with molecular clouds, the extension of the CR sources is important. In Section 2, taking into account the effect of a finite-size source, we first provide the distribution of CRs that have escaped from an SNR. Then, we consider the dynamical

★E-mail: ohira@post.kek.jp

evolution of CRs interacting with molecular clouds because the CR spectrum that has escaped from an SNR depends on the time evolution of the maximum energy (Ohira, Murase & Yamazaki 2010). In Sections 3 and 4 we provide two models of the evolution of the maximum energy. The gamma-ray spectra from molecular clouds are calculated in Section 5. Section 6 is devoted to a discussion.

2 DISTRIBUTION OF CRs ESCAPING FROM AN SNR

In this section, we derive the distribution of the runaway CRs at a given distance r from the SNR centre and at a given time t from the explosion time, $f(t, r, p)$, where p is the CR momentum. We here assume that the system is spherically symmetric and the diffusion coefficient in the interstellar medium $D_{\rm ISM}(p)$ is spatially uniform and depends on the CR momentum. Then, we solve the diffusion equation given by

$$\frac{\partial f}{\partial t}(t, r, p) - D_{\rm ISM}(p)\Delta f(t, r, p) = q_{\rm s}(t, r, p), \quad (1)$$

where $q_{\rm s}$ is the source term of CRs. Considering the escape process (Ptuskin & Zirakashvili 2005; Ohira et al. 2010), the CRs with a momentum p escape from an SNR at $t = t_{\rm esc}(p)$. The Green function, that is, the solution in the point-source case, $q_{\rm s} = N_{\rm esc}(p)\delta(\boldsymbol{r})\delta[t - t_{\rm esc}(p)]$, is (Atoyan, Aharonian & Völk 1995)

$$f_{\rm point}(t, r, p) = \frac{{\rm e}^{-\left(\frac{r}{R_{\rm d}(t,p)}\right)^2}}{\pi^{3/2} R_{\rm d}(t, p)^3} N_{\rm esc}(p), \quad (2)$$

where

$$R_{\rm d} = \sqrt{4D_{\rm ISM}(p)[t - t_{\rm esc}(p)]} \quad (3)$$

and

$$N_{\rm esc}(p) = \int {\rm d}t \int {\rm d}^3 r\; q_{\rm s}(t, r, p). \quad (4)$$

Now, taking into account the fact that the CRs escape from the SNR surface (Ohira et al. 2010), the source term is replaced with

$$q_{\rm s} = \frac{N_{\rm esc}(p)}{4\pi r^2}\delta[r - R_{\rm esc}(p)]\delta[t - t_{\rm esc}(p)], \quad (5)$$

where $R_{\rm esc}(p)$ is the radius where the CRs with momentum p escape from the SNR. Then, we find the solution to equation (1) as

$$f_{\rm ext}(t, r, p) = \int {\rm d}^3 r' f_{\rm point}(t, |\boldsymbol{r} - \boldsymbol{r}'|, p)\frac{\delta[r' - R_{\rm esc}(p)]}{4\pi r'^2}$$
$$= \frac{{\rm e}^{-\left(\frac{r - R_{\rm esc}(p)}{R_{\rm d}(t,p)}\right)^2} - {\rm e}^{-\left(\frac{r + R_{\rm esc}(p)}{R_{\rm d}(t,p)}\right)^2}}{4\pi^{3/2} R_{\rm d}(t, p) R_{\rm esc}(p) r} N_{\rm esc}(p). \quad (6)$$

Note that $f_{\rm ext}$ has a spectral break at $p = p_{\rm br,ext}$ because $f_{\rm ext} \approx N_{\rm esc}/4\pi^{3/2} R_{\rm d} R_{\rm esc} r$ for $r \sim R_{\rm esc} > R_{\rm d}$, otherwise $f_{\rm ext} \approx f_{\rm point}$, where $p_{\rm br,ext}$ is obtained from

$$R_{\rm esc}(p_{\rm br,ext}) = R_{\rm d}(p_{\rm br,ext}). \quad (7)$$

Below $p_{\rm br,ext}(R_{\rm esc} > R_{\rm d})$, the effect of a finite-size source becomes important. Recently, Li & Chen (2010) also considered the effect of a finite-size source.

The observed gamma-ray spectrum should be calculated by the volume-integrated CR spectrum. In the case of the SNR–molecular cloud interacting system, the emission region is a dense cloud or cavity wall, whose density is high in the region $L_1 \le r \le L_2$.

Considering the stellar wind before the supernova explosion, the inner radius of the molecular cloud L_1 is about a few tens of parsecs (Weaver, McCray & Castor 1977). The volume-integrated spectrum of CRs in the region $L_1 \le r \le L_2$ at the SNR age $t_{\rm age}$ is calculated as

$$F(p) = \int_{L_1}^{L_2} f_{\rm ext}(t_{\rm age}, r, p) 4\pi r^2 {\rm d}r. \quad (8)$$

Substituting equation (6) into equation (8), we obtain

$$F(p) = \frac{N_{\rm esc}(p)}{2}\left\{\frac{R_{\rm d}}{\sqrt{\pi}R_{\rm esc}}\left({\rm e}^{-\left(\frac{L_1 - R_{\rm esc}}{R_{\rm d}}\right)^2} - {\rm e}^{-\left(\frac{L_2 - R_{\rm esc}}{R_{\rm d}}\right)^2} - {\rm e}^{-\left(\frac{L_1 + R_{\rm esc}}{R_{\rm d}}\right)^2} + {\rm e}^{-\left(\frac{L_2 + R_{\rm esc}}{R_{\rm d}}\right)^2}\right) + {\rm erf}\left(\frac{L_2 - R_{\rm esc}}{R_{\rm d}}\right) - {\rm erf}\left(\frac{L_1 - R_{\rm esc}}{R_{\rm d}}\right) + {\rm erf}\left(\frac{L_2 + R_{\rm esc}}{R_{\rm d}}\right) - {\rm erf}\left(\frac{L_1 + R_{\rm esc}}{R_{\rm d}}\right)\right\}, \quad (9)$$

where ${\rm erf}(x) = (2/\sqrt{\pi})\int_0^x {\rm e}^{-y^2}{\rm d}y$ is the error function.

There are four characteristic momentum regimes determined by the comparison between the distances that CRs can reach, $R_{\rm esc}(p) + R_{\rm d}(p)$ and $L_{1,2}$ $[\ge R_{\rm esc}(p)]$, and that between $R_{\rm d}$ and $R_{\rm esc}$:

(i) $L_{1,2} < R_{\rm esc}(p) + R_{\rm d}(p)$ and $R_{\rm esc} < R_{\rm d}$,
(ii) $L_{1,2} < R_{\rm esc}(p) + R_{\rm d}(p)$ and $R_{\rm esc} > R_{\rm d}(L_1 \sim R_{\rm esc})$,
(iii) $L_1 < R_{\rm esc}(p) + R_{\rm d}(p) < L_2$,
(iv) $R_{\rm esc}(p) + R_{\rm d}(p) < L_{1,2}$.

Let us define $p_{\rm br,2}$ and $p_{\rm cut}$ as the solutions to the following equations:

$$L_2 = R_{\rm esc}(p_{\rm br,2}) + R_{\rm d}(p_{\rm br,2}) \quad (10)$$

$$L_1 = R_{\rm esc}(p_{\rm cut}) + R_{\rm d}(p_{\rm cut}). \quad (11)$$

We may expect $p_{\rm cut} < p_{\rm br,2}$ as long as the momentum dependence of $R_{\rm esc}$ is weak enough and/or $R_{\rm d}$ is more important. Then, a significant fraction of CRs with energies above $p_{\rm br,2}$ leave the molecular cloud, while CRs below $p_{\rm cut}$ do not essentially reach the cloud.

Furthermore, we approximate ${\rm e}^{-x^2} \approx 1 - x^2 + x^4/2$ and ${\rm erf}(x) \approx (2/\sqrt{\pi})(x - x^3/3)$ for $0 < x < 1$, and ${\rm e}^{-x^2} \approx 0$ and ${\rm erf}(x) \approx 1$ for $1 < x$. Then, for $p_{\rm br,ext} > p_{\rm br,2}$, we obtain

$$F(p) \propto N_{\rm esc}(p) \times \begin{cases} R_{\rm d}(p)^{-3} & (p > p_{\rm br,ext}) \\ R_{\rm d}(p)^{-1} R_{\rm esc}(p)^{-1} & (p_{\rm br,ext} > p > p_{\rm br,2}) \\ p^0 & (p_{\rm br,2} > p > p_{\rm cut}) \\ 0 & (p_{\rm cut} > p) \end{cases}. \quad (12)$$

For $p_{\rm br,2} > p_{\rm br,ext}$, we obtain

$$F(p) \propto N_{\rm esc}(p) \times \begin{cases} R_{\rm d}(p)^{-3} & (p > p_{\rm br,2}) \\ p^0 & (p_{\rm br,2} > p > p_{\rm cut}) \\ 0 & (p_{\rm cut} > p) \end{cases}. \quad (13)$$

Note that there is no break at $p_{\rm br,ext}$ since the effect of a finite-size source is smeared by spatial integration.

The spectral breaks at $p_{\rm br,ext}$ and $p_{\rm br,2}$ come from the finiteness of the source and the emission regions, respectively. To estimate the values of $p_{\rm br,2}$ and $p_{\rm cut}$, we first assume the diffusion coefficient of the interstellar medium,

$$D_{\rm ISM}(p) = 10^{28}\,\chi\left(\frac{cp}{10\,{\rm GeV}}\right)^{\delta}\ {\rm cm^2\,s^{-1}}, \quad (14)$$

where χ is constant. CR propagation models require $\chi \sim 1$ and $\delta \sim 0.5$ as the Galactic average value (Berezinskii et al. 1990). Assuming that $R_{\rm esc}$ and $t_{\rm esc}$ are constant with p (because the p-dependence of $R_{\rm esc}$ is weak), the typical value of $p_{\rm cut}$ is estimated as

$$p_{\rm cut} = 7 \left(\frac{\chi}{1}\right)^{-1/\delta} \left(\frac{L_1 - R_{\rm esc}}{5\,{\rm pc}}\right)^{2/\delta} \left(\frac{t - t_{\rm esc}}{10^4\,{\rm yr}}\right)^{-1/\delta} {\rm GeV}/c, \quad (15)$$

where we assume $\delta = 0.5$, and $p_{\rm br,2}$ is obtained by replacing L_1 with L_2. Although L_1 is of the order of 10 pc, *AGILE* observations show that a few $\times$ 100 MeV photons come from molecular clouds interacting with the SNR, that is, CRs with a few GeV energies have to reach the molecular clouds. In order for $p_{\rm cut}$ to be smaller than $\sim$1 GeV/c, $R_{\rm esc}$ should be of the order of L_1. Therefore, the effect of the finite-size source considered here is important. To estimate the values of those momentum breaks, we need to specify a model of $R_{\rm esc}(p)$. However, properties of particle escape depend on models. As we see in Section 4, when the whole SNR shell interacts with the molecular cloud, another momentum break $p_{\rm br,1}$ should be introduced, which plays a more crucial role than $p_{\rm cut}$.

Given $R_{\rm esc}(p), t_{\rm esc}(p)$ and $N_{\rm esc}(p)$, one can obtain $f_{\rm ext}(t, r, p)$ and $F(p)$. In Sections 3 and 4, we provide two models fixing $R_{\rm esc}(p), t_{\rm esc}(p)$ and $N_{\rm esc}(p)$ in the context of the SNR–molecular cloud interacting system.

3 MODEL 1: AN SNR INTERACTING WITH A SMALL MOLECULAR CLOUD

In this section, we consider the case in which a small part of an SNR shell interacts with a molecular cloud. In this case, the molecular cloud affects neither the dynamical evolution of the system nor the shock environments to confine CRs, so that both $R_{\rm esc}(p)$ and $N_{\rm esc}(p)$ are those for an isolated SNR which are obtained from Ohira et al. (2010). Here we briefly summarize the results of Ohira et al. (2010). In the framework of DSA, CRs are scattered by the turbulent magnetic field and go back and forth across the shock front. Once CRs reach far upstream where the shock front cannot be identified as a plane, the CRs cannot go back to the shock front, that is, the CRs escape from the SNR. In the context of DSA, the diffusion length of CR is $D(p)/u_{\rm sh}$, where $D(p)$ and $u_{\rm sh}$ are the diffusion coefficients in the vicinity of the shock and the shock velocity, respectively. The momentum of escaping CRs, $p_{\rm esc}$, is determined by

$$\frac{D(p_{\rm esc})}{u_{\rm sh}} \sim \ell_{\rm esc}, \quad (16)$$

where $\ell_{\rm esc}$ is the distance of the escape boundary from the shock front. We assume the Bohm-like diffusion coefficient $D = D_0 p$ and $\ell_{\rm esc} = \kappa R_{\rm sh}$ as a geometrical confinement condition, where we adopt $\kappa = 0.04$ throughout the paper (Ptuskin & Zirakashvili 2005). Then, we obtain

$$p_{\rm esc} = \kappa D_0^{-1} R_{\rm sh} u_{\rm sh}. \quad (17)$$

Although D_0 has not been understood in detail, $p_{\rm esc}$ starts to decrease when the Sedov phase begins at $t = t_{\rm Sedov}$. Hence we assume that CRs with the knee energy, $cp_{\rm knee} = 10^{15.5}$ eV, escape at $t = t_{\rm Sedov}$. We adopt a phenomenological approach based on the power-law dependence,

$$p_{\rm esc} = p_{\rm knee} \left(\frac{R_{\rm sh}}{R_{\rm Sedov}}\right)^{-\alpha}, \quad (18)$$

where $R_{\rm Sedov}$ is the SNR radius at $t = t_{\rm Sedov}$. We assume $\alpha = 6.5$ in order that $p_{\rm esc} = 1$ GeV/c at the end of the Sedov phase (Ohira et al. 2010).

From equations (17) and (18), we obtain

$$D_0 = \frac{\kappa R_{\rm sh} u_{\rm sh}}{p_{\rm knee}} \left(\frac{R_{\rm sh}}{R_{\rm Sedov}}\right)^{\alpha}. \quad (19)$$

Moreover, we assume that the number of CRs in the momentum range $(m_{\rm p}c, m_{\rm p}c + {\rm d}p)$ in the SNR is $K(R_{\rm sh})\,{\rm d}p \propto R_{\rm sh}^{\beta}$, where $m_{\rm p}$ is the proton mass, and that the CR spectrum at the shock front is p^{-s}. Then, in most of the cases, $N_{\rm esc}(p)$ has a single power-law form as

$$N_{\rm esc}(p) \propto p^{-(s+\beta/\alpha)}. \quad (20)$$

The value of β depends on the injection model and ranges from $-3/4$ to $3/13$ (Ohira et al. 2010). From equation (18), we derive

$$R_{\rm esc}(p) = (1+\kappa) R_{\rm Sedov} \left(\frac{p}{p_{\rm knee}}\right)^{-1/\alpha}. \quad (21)$$

Using the Sedov solution and equation (18), one finds

$$t_{\rm esc}(p) = t_{\rm Sedov} \left(\frac{p}{p_{\rm knee}}\right)^{-5/2\alpha}. \quad (22)$$

In this model, $R_{\rm esc}(p), t_{\rm esc}(p)$ and $N_{\rm esc}(p)$ obey single power laws, so that $F(p)$ is simply given by equations (12) or (13). For $p_{\rm br,ext} > p_{\rm br,2}$,

$$F(p) \propto \begin{cases} p^{-(1.5\delta+s+\beta/\alpha)} \Delta t(p)^{-3/2} & (p > p_{\rm br,ext}) \\ p^{-(0.5\delta+s+(\beta-1)/\alpha)} \Delta t(p)^{-1/2} & (p_{\rm br,ext} > p > p_{\rm br,2}) \\ p^{-(s+\beta/\alpha)} & (p_{\rm br,2} > p > p_{\rm cut}) \\ 0 & (p_{\rm cut} > p) \end{cases}. \quad (23)$$

For $p_{\rm br,2} > p_{\rm br,ext}$,

$$F(p) \propto \begin{cases} p^{-(1.5\delta+s+\beta/\alpha)} \Delta t(p)^{-3/2} & (p > p_{\rm br,2}) \\ p^{-(s+\beta/\alpha)} & (p_{\rm br,2} > p > p_{\rm cut}) \\ 0 & (p_{\rm cut} > p) \end{cases}, \quad (24)$$

where $\Delta\, t(p) = t - t_{\rm esc}(p)$.

4 MODEL 2: AN SNR EMBEDDED IN A MOLECULAR CLOUD

In this section, we consider the case in which the whole SNR shell interacts with the molecular clouds or cavity wall which are located at $L_1 < r < L_2$. Once the CRs encounter the molecular clouds, they all are expected to escape from the SNR because the high-density neutral gas damps plasma waves. In this case, the functional forms of $R_{\rm esc}(p)$ and $N_{\rm esc}(p)$ are different from those given in the previous section. At an early epoch, the SNR does not interact with the molecular clouds and $p_{\rm esc}$ is again determined by equation (16) with $\ell_{\rm esc} = \kappa R_{\rm sh}$. If the shock front gets closer to the molecular clouds and $L_1 - R_{\rm sh} < \kappa R_{\rm sh}$, $\ell_{\rm esc}$ should be replaced with $L_1 - R_{\rm sh}$. Therefore,

$$\ell_{\rm esc} = \min\left[\kappa R_{\rm sh}, L_1 - R_{\rm sh}\right]. \quad (25)$$

From equations (16), (19) and (25), we derive

$$p_{\rm esc} = p_{\rm knee} \left(\frac{R_{\rm sh}}{R_{\rm Sedov}}\right)^{-\alpha} \min\left[1, \frac{1}{\kappa}\left(\frac{L_1}{R_{\rm sh}} - 1\right)\right]. \quad (26)$$

The effective power-law index of $p_{\rm esc}$ at $R_{\rm sh} = L_1/(1+\kappa)$ is

$$-\left.\frac{{\rm d}\log p_{\rm esc}}{{\rm d}\log R_{\rm sh}}\right|_{R_{\rm sh}\to L_1/(1+\kappa)} = \alpha + 1 + \frac{1}{\kappa}. \quad (27)$$

Since $\kappa = 0.04$ is small, this index is much larger than α. This means that for $R_{\rm sh} > L_1/(1+\kappa)$, $p_{\rm esc}$ rapidly decreases. In other words, CRs with $p < p_{\rm br,1}$ escape at the same time at $t = t_{\rm Sedov}[L_1/(1+\kappa)R_{\rm Sedov}]^{5/2}$ and $p_{\rm br,1}$ is given by

$$p_{\rm br,1} = p_{\rm knee} \left(\frac{L_1}{R_{\rm Sedov}(1+\kappa)}\right)^{-\alpha}. \quad (28)$$

From equation (26), we find

$$R_{\rm esc}(p) = \begin{cases} (1+\kappa) R_{\rm Sedov} (p/p_{\rm knee})^{-1/\alpha} & (p > p_{\rm br,1}) \\ L_1 & (p \le p_{\rm br,1}) \end{cases} . \tag{29}$$

Using the Sedov solution and equation (26), we find

$$t_{\rm esc}(p) \approx \begin{cases} t_{\rm Sedov} (p/p_{\rm knee})^{-5/2\alpha} & (p > p_{\rm br,1}) \\ t_{\rm Sedov} \left(p_{\rm br,1}/p_{\rm knee}\right)^{-5/2\alpha} & (p \le p_{\rm br,1}) \end{cases} . \tag{30}$$

For $p < p_{\rm br,1}$, the spectrum of runaway CRs is the same as the CR spectrum at the shock because the CRs escape almost at the same time. Therefore, in this model, $N_{\rm esc}$ is approximately a broken power law,

$$N_{\rm esc}(p) \propto \begin{cases} p^{-(s+\beta/\alpha)} & (p > p_{\rm br,1}) \\ p_{\rm br,1}^{-\beta/\alpha} p^{-s} & (p \le p_{\rm br,1}) \end{cases} . \tag{31}$$

Generally speaking, the spectrum is complicated due to four breaks. However, in our cases almost all the CRs can reach the molecular cloud, where $F(p)$ essentially has three breaks at $p_{\rm br,ext}$, $p_{\rm br,1}$ and $p_{\rm br,2}$. If $p_{\rm br,2} < p < p_{\rm br,ext}$, then $F(p)/N_{\rm esc}(p)$ has a spectral break due to the break of $R_{\rm d}(p) R_{\rm esc}(p)$ (see equation 12). Keeping these in mind, we derive for $p_{\rm br,ext} > p_{\rm br,1} > p_{\rm br,2}$,

$$F(p) \propto \begin{cases} p^{-(1.5\delta+s+\beta/\alpha)} \Delta t(p)^{-3/2} & (p_{\rm br,ext} < p) \\ p^{-(0.5\delta+s+(\beta-1)/\alpha)} \Delta t(p)^{-1/2} & (p_{\rm br,1} < p < p_{\rm br,ext}) \\ p^{-(0.5\delta+s)} \Delta t(p)^{-1/2} & (p_{\rm br,2} < p < p_{\rm br,1}) \\ p^{-s} & (p < p_{\rm br,2}) \end{cases} ; \tag{32}$$

for $p_{\rm br,1} > p_{\rm br,ext} > p_{\rm br,2}$,

$$F(p) \propto \begin{cases} p^{-(1.5\delta+s+\beta/\alpha)} \Delta t(p)^{-3/2} & (p_{\rm br,1} < p) \\ p^{-(1.5\delta+s)} \Delta t(p)^{-3/2} & (p_{\rm br,ext} < p < p_{\rm br,1}) \\ p^{-(0.5\delta+s)} \Delta t(p)^{-1/2} & (p_{\rm br,2} < p < p_{\rm br,ext}) \\ p^{-s} & (p < p_{\rm br,2}) \end{cases} ; \tag{33}$$

for $p_{\rm br,1} > p_{\rm br,2} > p_{\rm br,ext}$,

$$F(p) \propto \begin{cases} p^{-(1.5\delta+s+\beta/\alpha)} \Delta t(p)^{-3/2} & (p_{\rm br,1} < p) \\ p^{-(1.5\delta+s)} \Delta t(p)^{-3/2} & (p_{\rm br,2} < p < p_{\rm br,1}) \\ p^{-s} & (p < p_{\rm br,2}) \end{cases} ; \tag{34}$$

for $p_{\rm br,ext} > p_{\rm br,2} > p_{\rm br,1}$,

$$F(p) \propto \begin{cases} p^{-(1.5\delta+s+\beta/\alpha)} \Delta t(p)^{-3/2} & (p_{\rm br,ext} < p) \\ p^{-(0.5\delta+s+(\beta-1)/\alpha)} \Delta t(p)^{-1/2} & (p_{\rm br,2} < p < p_{\rm br,ext}) \\ p^{-(s+\beta/\alpha)} & (p_{\rm br,1} < p < p_{\rm br,2}) \\ p^{-s} & (p < p_{\rm br,1}) \end{cases} \tag{35}$$

and for $p_{\rm br,2} > p_{\rm br,ext} > p_{\rm br,1}$ and $p_{\rm br,2} > p_{\rm br,1} > p_{\rm br,ext}$,

$$F(p) \propto \begin{cases} p^{-(1.5\delta+s+\beta/\alpha)} \Delta t(p)^{-3/2} & (p_{\rm br,2} < p) \\ p^{-(s+\beta/\alpha)} & (p_{\rm br,1} < p < p_{\rm br,2}) \\ p^{-s} & (p < p_{\rm br,1}) \end{cases} . \tag{36}$$

Note that when $p_{\rm br,1}$ is small enough, the model 2 is the same as model 1 except for $p_{\rm cut}$ [compare equations (23) with (35) or equations (24) with (36)].

5 GAMMA-RAY SPECTRUM FROM AN SNR

In this section, specifying model parameters, we calculate the gamma-ray spectrum from an SNR interacting with molecular clouds and compare it with the observed spectra.

We consider model 2, because observed spectra have no low-energy cut-off. From equations (3), (9), (14), (28), (29), (30) and (31), one can calculate the CR momentum spectrum. For simplicity, we assume that the injection model is the thermal leakage model, that is, $\beta = 3(3-s)/2$ (Ohira et al. 2010), $R_{\rm Sedov} = 2.1$ pc and $t_{\rm Sedov} = 210$ yr for all SNRs. Using the code provided by Kamae et al. (2006; see also Karlsson & Kamae 2008), we calculate the spectrum of π^0-decay gamma-rays. The normalization of the gamma-ray flux is adjusted to fit the data.

Figs 1–4 are the results for W51C, W28, W44 and IC 443, respectively. Table 1 is the list of adopted parameters and calculated break momentums. We find that for all SNRs, the observed gamma-ray breaks can be attributed to the momentum break at $p_{\rm br,1}$. For W51C and IC 443, the model predicts second breaks seen around 30 and 15 GeV, respectively (see Figs 1 and 4). For W51C, the break comes from the momentum break at $p_{\rm br,2}$, which is the effect of a finite-size emission zone, and for IC 443, the break comes from the momentum break at $p_{\rm br,ext}$, which is the effect of a finite-size source. Note

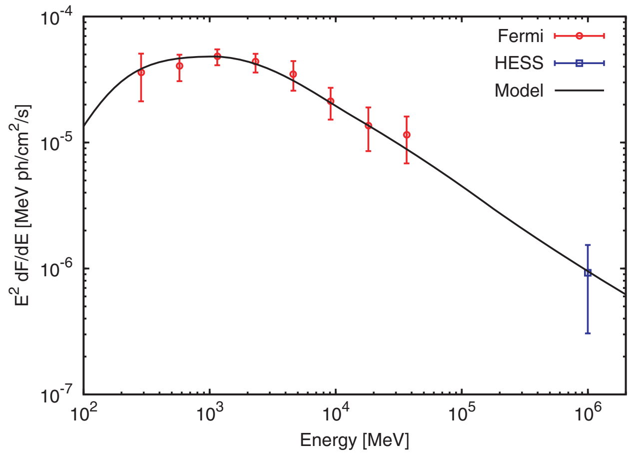

Figure 1. Comparison of the model results (solid line) with *Fermi* (red; Abdo et al. 2009b) and HESS (blue; Fiasson et al. 2009) observations for SNR W51C.

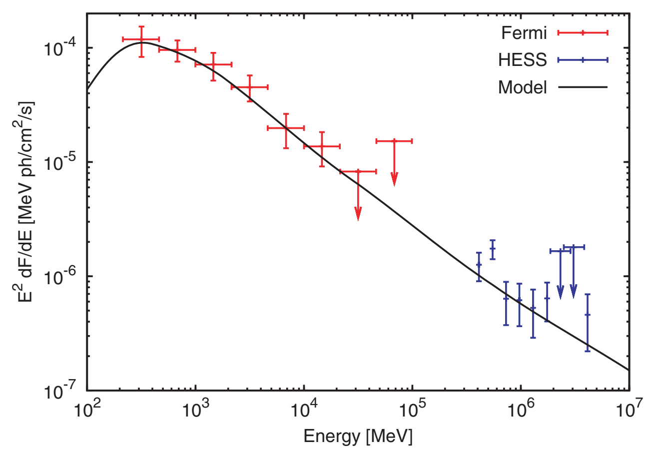

Figure 2. Comparison of the model results (solid line) with *Fermi* (red; Abdo et al. 2010b) and HESS (blue; Aharonian et al. 2008) observations for the source *N* of SNR W28.

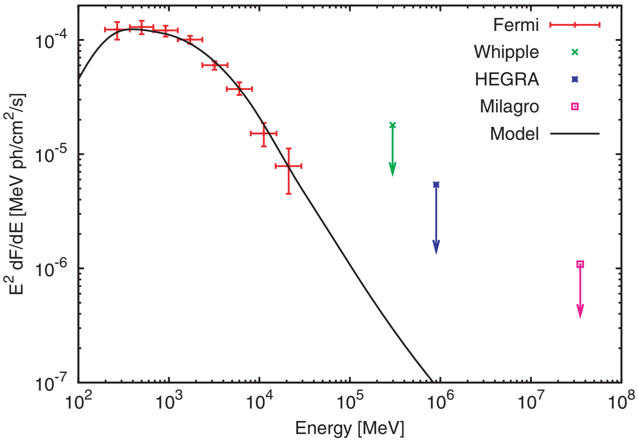

Figure 3. Comparison of the model results (solid line) with *Fermi* (red; Abdo et al. 2010c), Whipple (green; Buckley et al. 1998), HEGRA (blue; Aharonian et al. 2002 and Milagro (purple; Abdo et al. 2009a) observations for SNR W44. The data of Whipple, HEGRA and Milagro are upper limits.

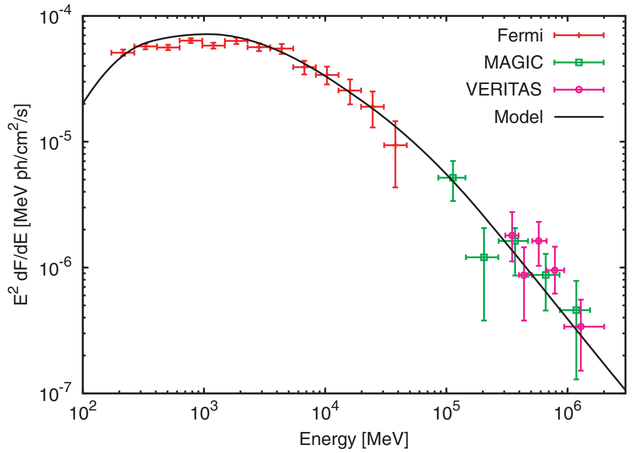

Figure 4. Comparison of the model results (solid line) with *Fermi* (red; Abdo et al. 2010a), MAGIC (green squares; Albert et al. 2007) and VERITAS (purple circles; Acciari et al. 2009) observations for SNR IC 443.

that $p_{\rm br,2}$ was also predicted by Aharonian & Atoyan (1996), while the other two breaks, $p_{\rm br,1}$ and $p_{\rm br,ext}$, are first introduced in this paper. For W28 and W44 (Figs 2 and 3), $p_{\rm br,2}$ and $p_{\rm br,ext}$ are much smaller than the threshold of the π^0 production, so that the spectrum is the same as that of the point-source solution (equation 2). Our model seems consistent with observations for all the SNRs. The observed data are fitted with the same parameters concerning the escape and the acceleration, α, β, κ and s. Hence, all the SNRs could have the same source spectrum above $p_{\rm br,1}(\sim 1$– $10\,{\rm GeV})$, required for explaining the Galactic CRs. The observed diversity of the gamma-ray spectra comes from five parameters related to CR propagation around SNRs (χ and δ) and/or environments (L_1, L_2 and $t_{\rm age}$).

6 DISCUSSION

For the four SNRs detected by *Fermi*, we have shown that they can be explained by an accelerated-CR spectrum with $s \approx 2.2$ and the corresponding runaway-CR spectrum with $s + \beta/\alpha \approx 2.38$. It is found that $s = 2.1$–2.4 also gives acceptable fits. Those spectral indices are consistent with those of the source spectrum of Galactic CRs, which is implied from GALPROP (Strong & Moskalenko 1998; Strong, Moskalenko & Reimer 2000) and others (e.g. Shibata et al. 2006; Putze et al. 2009), within uncertainties in the CR propagation. The inferred values are somewhat steeper than those predicted by the classical DSA ($s = 2$), and several mechanisms have been proposed to explain such steeper spectra (Kirk, Duffy & Gallant 1996; Zirakashvili & Ptuskin 2008; Fujita et al. 2009; Ohira, Terasawa & Takahara 2009b; Ohira & Takahara 2010). However, our results are based on several approximations, and we have investigated only four middle-aged SNRs, so that results on indices are not conclusive yet. Further theoretical and observational studies are obviously required in order to discuss underlying acceleration mechanisms and reveal the link between those middle-aged SNRs and the observed Galactic CRs.

In order to fit the data, the parameters concerning the diffusion coefficient of CRs just around the SNR, χ and δ, are different from the Galactic mean values, $\chi \sim 1$ and $\delta \sim 0.5$ (see Table 1). A possible explanation of these discrepancies is that the runaway CRs amplify the magnetic fluctuation, so that the diffusion coefficient in the medium with high CR density can be different from the Galactic average. The higher the CR density is, the more turbulent the magnetic field, and the more frequent the scattering of CRs, resulting in a smaller diffusion coefficient. On the other hand, the magnetic turbulence becomes weak if the neutral particles impede the magnetic field amplification. Further studies are needed to understand the physics of partially ionized interstellar matter illuminated by CRs.

Some important processes neglected so far should be mentioned. First, in Section 2, the diffusion coefficient of CRs in the interstellar medium, $D_{\rm ISM}(p)$, is assumed to be spatially uniform and time-independent. Fujita, Ohira & Takahara (2010) demonstrated that CRs that have escaped from an SNR excite plasma waves and reduce the diffusion coefficient (Kulsrud & Pearce 1969; Wentzel 1969; Ptuskin, Zirakashvili & Plesser 2008), which is responsible for a non-uniform, time-dependent diffusion coefficient. Secondly, in Sections 3 and 4, we assume the diffusion coefficient just around the shock has the form of equation (19). Although the magnetic field amplification around the shock has been studied by linear analysis (Bell 2004; Reville et al. 2007; Ohira et al. 2009b) and many numerical simulations (Lucek & Bell 2000; Giacalone & Jokipii 2007; Niemiec, Polh & Nishikawa 2008; Reville et al. 2008; Inoue, Yamazaki & Inutsuka 2009; Ohira et al. 2009a; Riquelme &

Table 1. Model parameters and characteristic momentums.

SNR	α	β	κ	s	δ	χ	L_1 (pc)	L_2 (pc)	$t_{\rm age}$ (kyr)	$p_{\rm br,1}$ (GeV/c)	$p_{\rm br,2}$ (GeV/c)	$p_{\rm br,ext}$ (GeV/c)
W51C	6.5	1.2	0.04	2.2	0.22	0.1	14.7	23.7	31.5	13.1	124	21.6
W28	6.5	1.2	0.04	2.2	0.19	0.9	18.5	26.9	63.0	2.96	<1.43	<1.43
W44	6.5	1.2	0.04	2.2	0.40	1.0	12.4	16.2	23.1	39.8	<1.43	<1.43
IC 443	6.5	1.2	0.04	2.2	0.62	0.01	11.5	14.7	23.1	62.9	2.93	151

Spitkovsky 2009; Vladimirov, Bykov & Ellison 2009), the saturation of the magnetic field amplification and the diffusion coefficient has not yet been understood in detail. Finally, in Sections 3 and 4, we assume that the CR spectrum at the shock has a single power law, p^{-s}, at any time. However, the situation may not be so simple. The shock compression ratio decreases as the shock velocity decreases. As a result, the spectrum becomes steeper with time (Fujita et al. 2009). In addition, neutral particles have great impacts on the magnetic field and the particle acceleration (Ohira et al. 2009b; Ohira & Takahara 2010). Moreover, non-linear DSA should be considered when CRs affect the shock structure (Drury & Völk 1981; Malkov & Drury 2001), along with properties of magnetic turbulence in magnetic field amplification (Vladimirov et al. 2009). Further studies are needed to clarify the significance of these effects.

ACKNOWLEDGMENTS

We thank Y. Fujita, F. Takahara, K. Kohri and T. Kamae for useful discussion. This work is supported in part by grant-in-aid from the Ministry of Education, Culture, Sports, Science and Technology (MEXT) of Japan, no. 21684014 (YO), nos 19047004, 21740184 and 21540259 (RY).

REFERENCES

Abdo A. A. et al., 2009a, ApJ, 700, L127
Abdo A. A. et al., 2009b, ApJ, 706, L1
Abdo A. A. et al., 2010a, ApJ, 712, 459
Abdo A. A. et al., 2010b, ApJ, 718, 348
Abdo A. A. et al., 2010c, Sci, 327, 1103
Acciari V. A. et al., 2009, ApJ, 698, L133
Aharonian F. A., Atoyan A., 1996, A&A, 309, 917
Aharonian F. A. et al., 2002, A&A, 395, 803
Aharonian F. A. et al., 2008, A&A, 481, 401
Albert J. et al., 2007 ApJ, 664, L87
Atoyan A. M., Aharonian F. A., Völk H. J., 1995, Phys. Rev. D, 52, 3265
Axford W. I., Leer E., Skadron G., 1977, in Proc. 15th Int. Cosmic Ray Conf., Plovdiv, Vol. 11. Bulgarian Academy of Science, Plovdiv, p. 132
Baade W., Zwicky F., 1934, Proc. Natl. Acad. Sci., 20, 259
Bell A. R., 1978, MNRAS, 182, 147
Bell A. R., 2004, MNRAS, 353, 550
Berezinskii V. S., Bulanov S. V., Dogiel V. A., Ginzburg V. L., Ptuskin V. S., 1990, Astrophysics of Cosmic Rays. North Holland, Amsterdam
Blandford R. D., Ostriker J. P., 1978, ApJ, 221, L29
Buckley J. H. et al., 1998, A&A, 329, 639
Drury L. O'C., Völk H. J., 1981, ApJ, 248, 344
Fiasson A., Marandon V., Chaves R. J. G., Tibolla O. (HESS collaboration) 2009, in Proc. 31st Int. Cosmic Ray Conf., in press
Fujita Y., Ohira Y., Tanaka S. J., Takahara F., 2009, ApJ, 707, L179
Fujita Y., Ohira Y., Takahara F., 2010, ApJ, 712, L153
Gabici S., Aharonian F. A., Casanova S., 2009, MNRAS, 369, 1629
Giacalone J., Jokipii J. R., 2007, ApJ, 663, L41
Giuliani A. et al., 2010, A&A, 516, L11
Inoue T., Yamazaki R., Inutsuka S., 2009, ApJ, 695, 825
Kamae T., Karlsson N., Mizuno T., Abe T., Koi T., 2006, ApJ, 647, 692
Karlsson N., Kamae T., 2008, ApJ, 674, 278
Kirk J. G., Duffy P., Gallant Y. A., 1996, A&A, 314, 1010
Kulsrud R. M., Pearce W. P., 1969, ApJ, 156, 445
Krymsky G. F., 1977, Doklady Akademii Nauk SSSR, 234, 1306
Li H., Chen Y., 2010, MNRAS, in press (arXiv:1009.0894)
Lucek S. G., Bell A. R., 2000, MNRAS, 314, 65
Malkov M. A., Drury L. O'C., 2001, Rep. Progress Phys., 64, 429
Malkov M. A., Diamond P. H., Sagdeev R. Z., 2010, preprint (arXiv:1004.4714)
Niemiec J., Polh M., Nishikawa K., 2008, ApJ, 684, 1174
Ohira Y., Takahara F., 2010, ApJ, 721, L43
Ohira Y., Reville B., Kirk J. G., Takahara F., 2009a, ApJ, 698, 445
Ohira Y., Terasawa T., Takahara F., 2009b, ApJ, 703, L59
Ohira Y., Murase K., Yamazaki R., 2010, A&A, 513, A17
Ptuskin V. S., Zirakashvili V. N., Plesser A. A., 2008, Advances Space Res., 42, 486
Ptuskin V. S., Zirakashvili V. N., 2005, A&A, 429, 755
Putze A., Derome L., Maurin D., Perotto L., Taillet R., 2009, A&A, 497, 991
Riquelme M. A., Spitkovsky A., 2009, ApJ, 694, 626
Reville B., Kirk J. G., Duffy P., O'Sullivan S., 2007, A&A, 475, 435
Reville B., O'Sullivan S., Duffy P., Kirk J. G., 2008, MNRAS, 386, 509
Shibata T., Hareyama M., Nakazawa M., Saito C., 2006, ApJ, 642, 882
Strong A. W., Moskalenko I. V., 1998, ApJ, 509, 212
Strong A. W., Moskalenko I. V., Reimer O., 2000, ApJ, 537, 763
Tavani M. et al., 2010, ApJ, 710, L151
Vladimirov A. E., Bykov A. M., Ellison D. C., 2009, ApJ, 703, L29
Weaver R., McCray R., Castor J., 1977, ApJ, 218, 377
Wentzel D. G., 1969, ApJ, 156, 303
Zirakashvili V. N., Ptuskin V. S., 2009, in Aharonian F. A., Hofmann W., Rieger F. M. eds, AIP Conf. Proc. Vol. 1085, High Energy Gamma-Ray Astronomy, Am. Inst. Phys., New York, p. 336

This paper has been typeset from a TEX/LATEX file prepared by the author.